

Simulation for 3-dimensional optical and electrical analysis of CCD

Hideki Mutoh

Link Research Corporation

1-18-5, Kojima, Taito-ku, Tokyo, 111 Japan

Phone: +81-3-3851-9871

Fax: +81-3-3862-0570

E-Mail: tbc00514@niftyserve.or.jp

Abstract: A device simulator SPECTRA and a topography and optics simulator TOCCATA were developed for 3-dimensional optical and electrical analysis of CCD. SPECTRA solves Poisson's and time dependent current continuity equations by a novel Gummel's method. Since the basic parameters are potential and exponential functions of quasi-Fermi level of electron and hole, the solution is obtained more stably and rapidly than the conventional method. TOCCATA calculates the shape of layers formed on a silicon substrate and performs ray tracing on multiple reflection, refraction, and absorption. The combination of these simulators enables the total design of CCD cell structures on and in a silicon substrate. Optical and electrical characteristics of a 1/4 inch 380K pixel IL-CCD were studied. It was found that the sensitivity and smear dependence on incident light angle increases with the increase of the micro lens focal length.

I. Introduction

The reduction of pixel size of CCD image sensors has been a main trend because of the demand for cheap and compact video equipment. Three-dimensional device simulation has been utilized to develop new and complicated structures such as fully-depleted buried photo-diodes without image lag, vertical overflow drains with an electronic shutter function, and dual horizontal CCD with high charge transfer efficiency [1]. In addition to the electrical characteristics analysis, optical characteristics analysis becomes important with the reduction of pixel size because a micro lens structure is needed to enhance the sensitivity of small pixel size CCD image sensors. For realizing such analysis, a 3-dimensional device simulator SPECTRA and a 3-dimensional topography and optics simulator TOCCATA were developed. This combination enables the total design of CCD cell structures on and in a silicon substrate. The analysis of the electrical and optical characteristics of a 1/4 inch 380K pixel IL-CCD is reported.

II. Modeling

A. Device simulation

A summary of the device simulation models is shown in Table 1. A time dependent drift diffusion model is adopted. Since the basic parameters are potential and exponential functions of quasi-Fermi level of electron and hole, the stability and speed of matrix calculations are better than conventional simulators whose basic parameters are potential and concentrations of electrons and holes. When exponential functions of quasi-Fermi level of electron and hole are basic parameters, the current continuity equation matrices are symmetric and it is possible to use ICCG method [3] which is the fastest and most stable method for matrix calculations. Periodic or reflective horizontal boundary conditions can be chosen. This is an important feature for devices whose cells are arranged periodically such as CCD image sensors.

Table 1 Summary of device simulation models

basic model	time dependent drift diffusion model
basic parameter	potential and exponential function of quasi-Fermi level
discretization	finite differential method
boundary condition	periodic or reflective
solving scheme	Gummel's method [2]
matrix solver	SOR and ICCG

B. Topography simulation

Topography simulation is executed by calculating the Z-coordinate of the interface grid points whose X- and Y-coordinate are initially defined. When the coordinate of the i-th grid point of a n-th layer is $(x_i, y_i, z_{n,i})$, $z_{n,i}$ is

described by

$$z_{n,i} = \begin{cases} \max [z_{n-1,j} + \sqrt{t_n^2 - \alpha^2 \{(x_i - x_j)^2 + (y_i - y_j)^2\}}] & : \text{ in the defined region} \\ z_{n-1,i} & : \text{ out of the defined region} \end{cases}$$

where t_n is the thickness of the n-th layer, α is a structure parameter, and x_j and y_j are the grid coordinates which satisfy $(x_i - x_j)^2 + (y_i - y_j)^2 < t_n^2 \alpha^2$.

Micro lens structures can be described by user defining functions.

C. Optics simulation

Ray tracing based on Snell's law and Fresnel's equations is performed with multiple reflection, refraction, and absorption. Random polarization is assumed at every reflection and refraction.

Incident light angle θ_1 , refractive light angle θ_2 , refractive indices n_1 and n_2 , averaged energy reflectance R, and transmittance T satisfy the following equations.

$$n_2 \sin \theta_2 = n_1 \sin \theta_1$$

$$R = \frac{1}{2} \left\{ \frac{\tan^2(\theta_2 - \theta_1)}{\tan^2(\theta_2 + \theta_1)} + \frac{\sin^2(\theta_2 - \theta_1)}{\sin^2(\theta_2 + \theta_1)} \right\}, \quad T = \frac{1}{2} \left\{ \frac{\sin 2\theta_2 \sin 2\theta_1}{\sin^2(\theta_2 + \theta_1) \cos^2(\theta_2 - \theta_1)} + \frac{\sin 2\theta_2 \sin 2\theta_1}{\sin^2(\theta_2 + \theta_1)} \right\}$$

III. Analysis of a 1/4 inch 380K pixel CCD

Fig. 1 shows the cell structure of a 1/4 inch 380K pixel CCD. The cell size is $4.75 \mu\text{m}$ (H) x $5.55 \mu\text{m}$ (V) and the maximum depth of the simulation region is $15 \mu\text{m}$. Two level poly-silicon, two level aluminum, and a micro-lens process are assumed. Figs. 2 and 3 show the maximum potential during normal operation in the XZ- and XY-planes, respectively. The maximum potential during electronic shutter and read out operations are shown in Figs. 4 and 5, respectively.

Fig. 6 shows the electron current in a saturation condition. The maximum storage charge of the photo-diode can be estimated by integrating electron concentration around the photo-diode region.

The time dependence of VCCD transfer inefficiency is shown in Fig. 7. It is found that charge transfer between the potential wells under two adjacent gates takes place in 1 ns.

A cross-sectional view in the XZ-plane of the cell structure with a micro lens on XZ-plane is shown in Fig. 8. Sensitivity and smear characteristics of three kinds of micro lens structure whose focal lengths are 2, 4, and $6 \mu\text{m}$ are studied. Figs. 9 and 10 show the incident light angle dependencies. It is found that the sensitivity and smear of longer focal length structures are more sensitive to the incident angle variations. Fig. 11 shows ray tracing of micro lens structures when the incident light angle is 10 degrees. The features of Figs. 9 and 10 are explained by the fact that the focal point shift caused by the oblique incident light increases with the increase of the focal length of micro lens.

IV. Conclusion

Novel simulation methods for the 3-dimensional optical and electrical analysis of CCD were developed. This enables the total design of CCD cell structures on and in a silicon substrate. The optical and electrical characteristics of a 1/4 inch 380K pixel IL-CCD was studied by this method. Potential profiles during electronic shutter and read out operations, current distribution in saturation condition, VCCD transfer efficiency, and sensitivity and smear characteristics were analyzed. It was found that the sensitivity and smear dependence on incident light angle increases with the increase of the micro lens focal length.

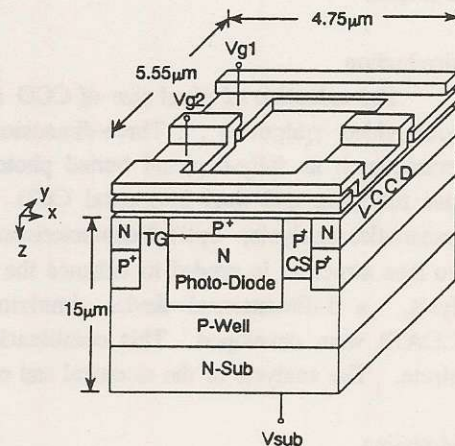


Fig. 1 1/4 inch 380K pixel CCD cell structure.

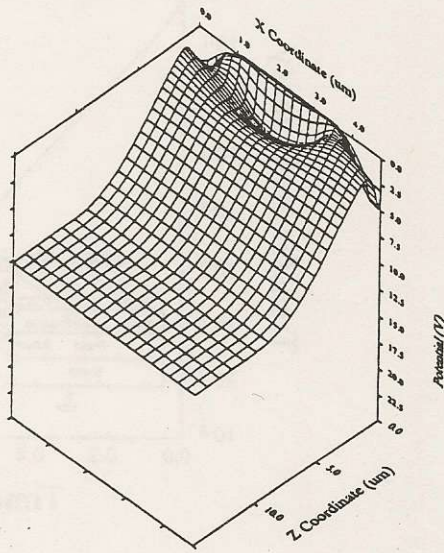


Fig. 2 Maximum potential during normal operation in the XZ-plane ($V_{g1}=0, V_{g2}=0, V_{sub}=10$).

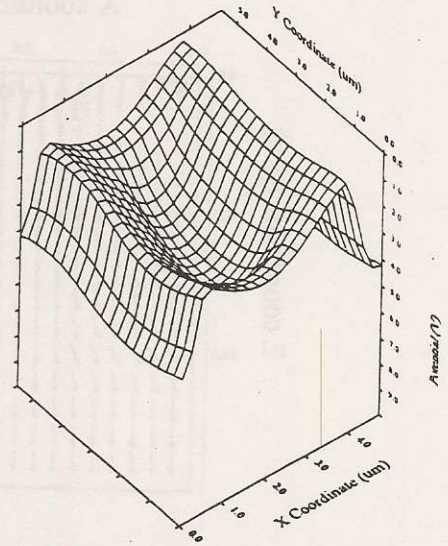


Fig. 3 Maximum potential during normal operation in the XY-plane ($0 \leq Z \leq 0.15, V_{g1}=0, V_{g2}=0, V_{sub}=10$).

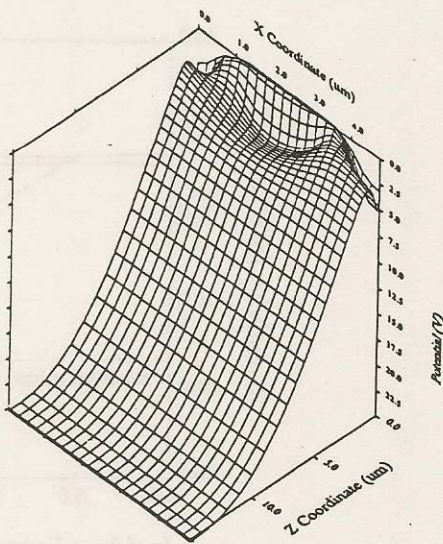


Fig. 4 Maximum potential during electronic shutter operation in the XZ-plane ($V_{g1}=0, V_{g2}=0, V_{sub}=25$).

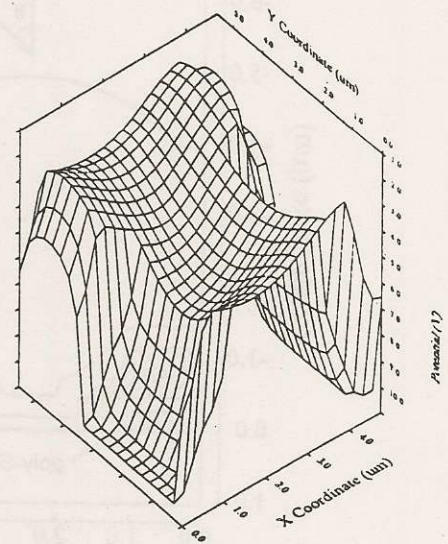


Fig. 5 Maximum potential during read out operation in the XY-plane ($0 \leq Z \leq 0.15, V_{g1}=0, V_{g2}=10, V_{sub}=10$).

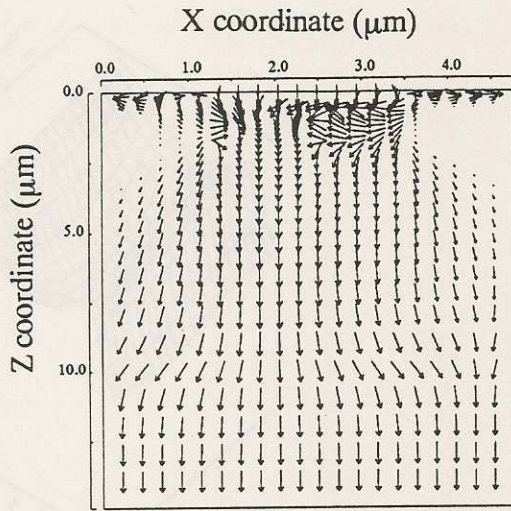


Fig. 6 Electron current in a saturation condition in the XZ plane ($y=2.7$, $V_{g1}=0$, $V_{g2}=0$, $V_{sub}=10$).

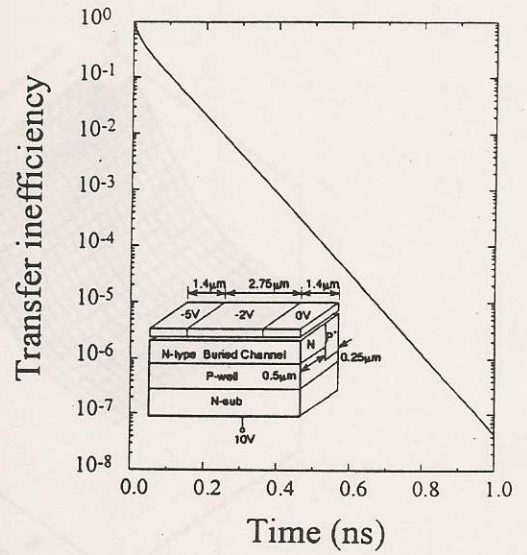


Fig. 7 Time dependence of VCCD transfer inefficiency.

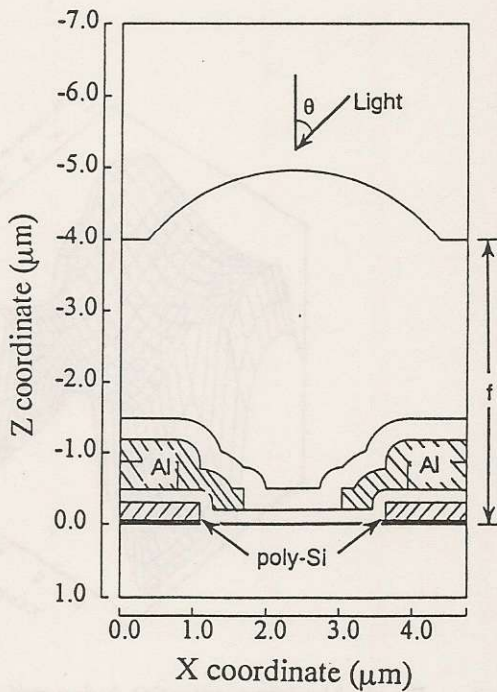


Fig. 8 Cross-sectional view in the XZ-plane of cell structure with micro lens. θ is the incident light angle.

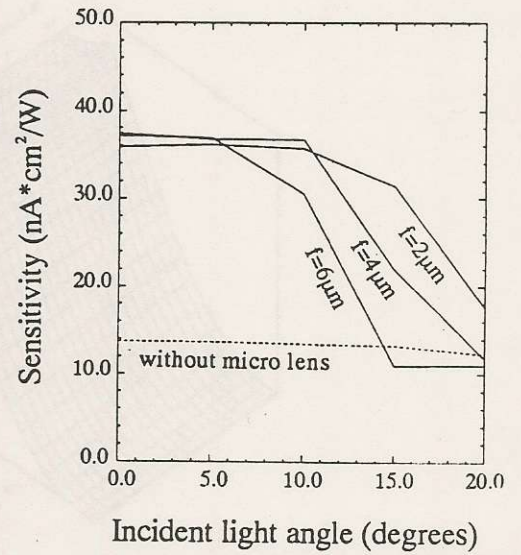


Fig. 9 Sensitivity dependence on incident light angle and micro lens focal length (f).

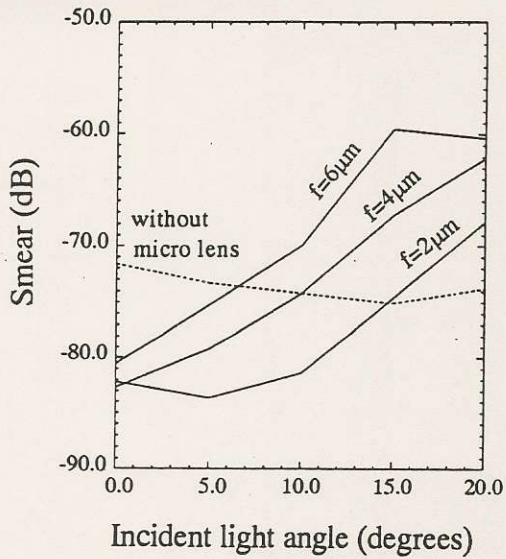


Fig. 10 Smear dependence on incident light angle and micro lens focal length (f).

References

- [1] H. Mutoh et al., "A 2/3 inch 800k Pixel Color Image Sensor," ITEJ Technical Report, vol. 13, No. 11, pp. 73-78, TEBS '89-13, ED '89-17, Feb. 1989.
- [2] S. Selberherr, *Analysis and Simulation of Semiconductor Devices*, Springer-Verlag, pp. 208-212, 1984.
- [3] D. S. Kershav, "The Incomplete Cholesky Conjugate Gradient Method for the Iterative Solution of Systems of Linear Equations," *J. Comp. Phys.*, vol. 26, pp. 43-65, 1978.

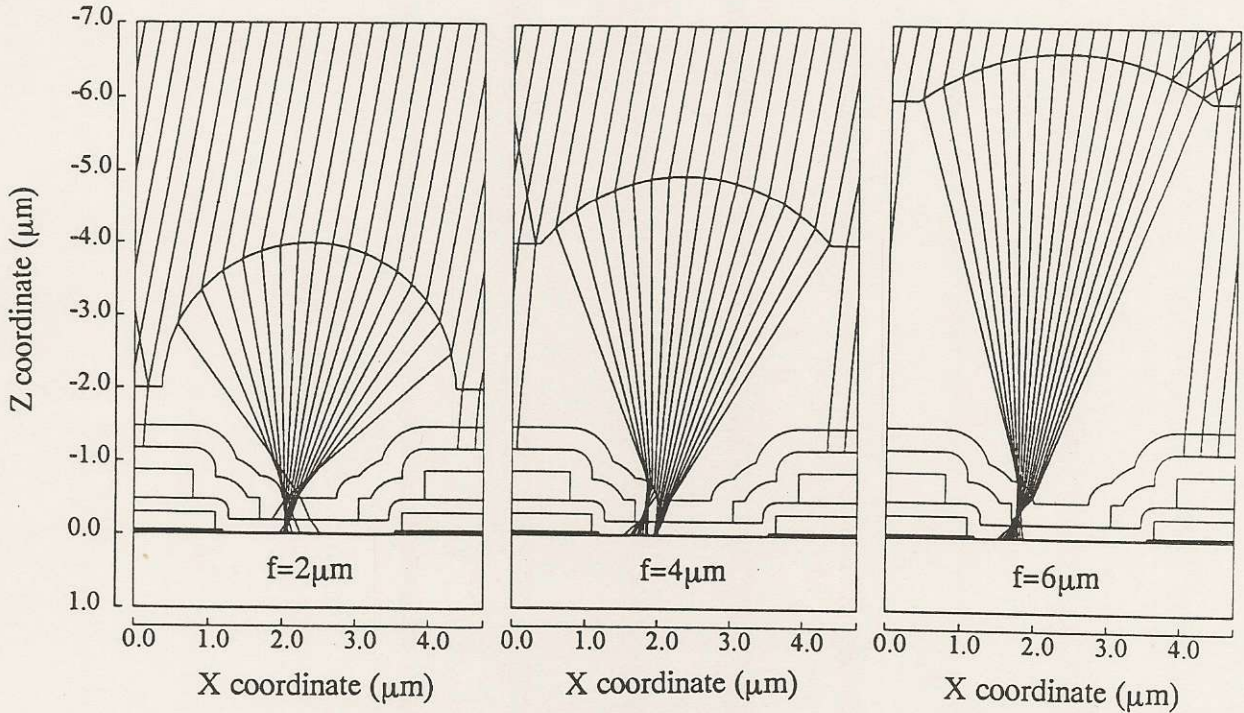


Fig. 11 Ray tracing of micro lens structures. Incident light angle is 10 degrees.